



SPE/ISRM 47243

## Flexurally-Induced Stresses in the Northern North Sea: Preliminary Comparison of Observation and Theory

B. Grollmund, M. D. Zoback, SPE, Dept. of Geophysics, Stanford University, and L. Arnesen, Norsk Hydro

Copyright 1998, Society of Petroleum Engineers, Inc.

This paper was prepared for presentation at SPE/ISRM Eurock '98 held in Trondheim, Norway, 8-10 July 1998.

This paper was selected for presentation by an SPE Program Committee following review of information contained in an abstract submitted by the author(s). Contents of the paper, as presented, have not been reviewed by the Society of Petroleum Engineers and are subject to correction by the author(s). The material, as presented, does not necessarily reflect any position of the Society of Petroleum Engineers, its officers, or members. Papers presented at SPE meetings are subject to publication review by Editorial Committees of the Society of Petroleum Engineers. Electronic reproduction, distribution, or storage of any part of this paper for commercial purposes without the written consent of the Society of Petroleum Engineers is prohibited. Permission to reproduce in print is restricted to an abstract of not more than 300 words; illustrations may not be copied. The abstract must contain conspicuous acknowledgment of where and by whom the paper was presented. Write Librarian, SPE, P.O. Box 833836, Richardson, TX 75083-3836, U.S.A., fax 01-972-952-9435.

### Abstract

In this work we evaluate the role of lithospheric flexure resulting from post-glacial rebound as a possible source of regional stress variations in the northern North Sea. Compilations of leak-off and pore pressure data, estimates of the full stress tensor from observations of wellbore failure<sup>1</sup>, and earthquake focal plane mechanisms indicate high horizontal compression (i.e.,  $S_{Hmax} > S_V$  and  $S_{Hmin} \sim S_V$ ) on the west side of the Viking Graben and decreased horizontal stresses on the east side. In this study we extend the available knowledge about regional stress magnitudes by analysis of leak-off and pore pressure data. We use numerical modeling of lithospheric flexure due to post glacial rebound to show that this is a possible cause of the observed high horizontal compression in the Tampen Spur, regional stress variations and possibly the high pore pressures observed at depth west of the Viking Graben.

### Introduction

In this paper we investigate one specific mechanism, post-glacial lithospheric flexure, that may contribute to high horizontal stresses observed in the Tampen Spur area of the northern North Sea. More generally, it's important to understand if lithospheric flexure resulting from deglaciation is responsible for regional variations of stress orientations<sup>2,3</sup> and magnitude<sup>4</sup> which in turn may affect reservoir processes as diverse as wellbore stability and hydrocarbon migration.

We analyzed leak-off and pore pressure data in the northern North Sea to document values at depth and to reveal spatial and depth dependent changes. These data supplement information from earthquake focal plane mechanisms<sup>5</sup>, and

estimates of the full stress tensor in the Visnes field.

Further, we use numerical modeling to explain the observed stresses. While numerical modeling of stress in the North Sea has already been carried out, which resulted in a good first-order approximation of the regional stress field, the effect of Quaternary deglaciation on the Fennoscandian shield due to deglaciation was not included in the model. Since we believe that this might be an important source of stress in the northern North Sea we present a numerical model involving flexural stresses due to deglaciation.

### Observation of Stress in the Northern North Sea

To determine stress regimes in the northern North Sea we analyzed leak-off tests from wells located in the northern North Sea as well as from wells closer to the Norwegian coast. The least principal stress ( $S_3$ ) approaches the vertical stress regime is likely to be compressive, horizontal stress ( $S_{Hmax}$ ) is higher than  $S_V$ , and  $S_{Hmin}$  is significantly lower than  $S_V$ , the stress state is slip/reverse faulting. Thus leak-off tests can be valuable to determine approximate state of stress.

To map spatial changes of stress we use leak-off test results normalized by  $S_V$  deduced from density logs. The ratio  $S_3/S_V$  along the cross section perpendicular to the Norwegian coast. At depths between 1,000 m and 1,500 m,  $S_3/S_V$  is very small. At 3,000 m  $S_3/S_V$  tends to decrease towards the coast. In the Snorre field,  $S_3$  is almost equal to  $S_V$ , indicating a slip/reverse faulting stress state. At the same depth  $S_3/S_V$  is considerably lower in block 35/9, which indicates a slip/normal faulting stress state in this area.

Since leak-off tests only reveal the maximum principal stress, complete determination of stress, based on leak-off tests is impossible. A study of the full stress tensor and observations of wellbore failure<sup>1</sup> is needed to determine the wellbore failure it is known that in the Visnes field values between 1.2 and 1.3 at depths between 1,000 and 3,500 m. Together with the leak-off data, this indicates a slip faulting regime with  $S_3$  being very close to  $S_V$  and  $S_{Hmax}$  considerably higher than  $S_V$  (Fig. 2).

Earthquake data<sup>5</sup> indicate a predominant strike-slip stress state in the Tampen Spur with a tendency towards slip faulting closer to the coast (Fig. 1). However,

the earthquake data is poor, and the depth range of the earthquakes is unknown.

Fig. 3 shows the pore pressure, normalized by the vertical stress ( $P_p/S_v$ ).  $P_p/S_v$  is a measure for how strongly a formation is overpressured. To a depth of approximately 1,500 m  $P_p/S_v$  is close to 0.5, which means that the pore pressure is hydrostatic along the entire cross section. In block 35/9 the pore pressure remains close to hydrostatic to a depth of 3,000 m. On the other hand in the Tampen Spur area, severe overpressure starts at a much shallower depth of 2,000 m.

In general, all available data agree that the stress field is reverse/strike-slip faulting in the vicinity of the Tampen Spur. Closer to the coast though,  $S_3$  seems to be considerably lower than  $S_v$  and the stress field appears to be less compressive although the distribution of earthquake focal mechanisms indicate a strike-slip/reverse stress regime in both areas. Importantly, pore pressure is considerably higher in the Tampen Spur than east of the Viking Graben, e.g. block 35/9.

**Modeling Flexural Stresses due to Glacial Loading**

Stresses in the northern North Sea are likely caused by a number of mechanisms. Several studies have pointed out the importance of ridge push along the entire Norwegian Margin<sup>2,6</sup>. Since the crust cools down and becomes denser as it moves away from the Mid Atlantic Ridge, gravitational sliding occurs and causes high stresses in the direction of plate motion<sup>7,8</sup>. The observation that  $S_{Hmax}$  directions along the Norwegian Margin are more or less parallel to the direction of plate motion<sup>5</sup> indicates the importance of ridge push as a large scale stress source. Observed stress variations in the northern North Sea however, suggest that there are other factors that locally affect the stress field.

In this work we've investigated the importance of flexural stresses caused by glaciation. Fig. 4 illustrates how glaciation might perturb the stress field. In Fig. 4a we assume that the lithosphere has reached a state of equilibrium before the ice sheet started to melt. At shallow depth, subsequent ice melting causes extension under the ice sheet, and offshore compression. At great depth this effect is reversed. Stein et al.<sup>9</sup> have used this concept to model flexural stress in the Baffin Bay region in Canada to explain the occurrence of a large reverse faulting earthquake at shallow depth in 1933. In Fig. 4b the lithosphere is expected to store flexural stresses over long periods of time. Therefore, flexural stresses at shallow depth are always compressive under the ice sheet, and extensional further offshore<sup>10</sup> approaching an isotropic stress state after the melting of the ice sheet. This however is not consistent with the observed spatial stress variations.

**Analytical Model.** To get an estimate of the magnitude of stress changes due to glaciation we initially developed a simple two-dimensional analytical model along the cross section shown in Fig. 1. This model assumes the case of Fig. 4a where the lithosphere is fully relaxed before the onset of ice melting. The lithosphere is represented by an elastic plate, and the ice sheet is assumed to have a constant thickness of 1 km with the lateral extent from 15,000 years ago. For these

assumptions flexural stresses can be calculated using conventional formulae for elastic plate flexure.

At shallow depth the model predicts compressive stresses on the order of 20 MPa in the vicinity of Visund. Closer to the coast flexural stresses are on the order of -20 MPa (Fig. 5a). The stress perturbation is approximately 200 km thick because of the thickness of the stress supporting lithosphere suggested by Carter and Tsenn<sup>12</sup>, which matches the stress variations very well. Fig. 5b illustrates the decrease of flexural stresses with depth.

It can be concluded that the analytical model is a good order approximation of the observed stress variations in the northern North Sea, and suggests that deglaciation has a significant influence on the local stress field. The model's usefulness is limited since shape and thickness of the ice sheet are strongly simplified. Furthermore, the purely elastic lithosphere is questionable since viscoplastic deformation in the upper crust, and viscoplastic flow in the lower crust and the mantle are likely to occur<sup>13</sup>.

**Numerical Model.** To explore the effect of viscoplasticity in the lithosphere with a more realistic rheology we developed a two-dimensional finite-element model. The use of this model also allows the ice sheet to gradually melt rather than removed instantaneously.

Fig. 6a shows the lithospheric model. The model is divided into a brittle and a ductile part. The brittle part is a 10 km thick sediment layer, underlain by 15 km of lithosphere. The model uses Mohr-Coulomb plasticity to account for the behavior of the upper crust (Eq. 1).

$$\sigma_1 = \sigma_3[(\mu^2+1)^{0.5} + \mu]^2 + C_0$$

We are assuming a coefficient of friction  $\mu$  of 0.5 and a cohesion ( $C_0$ ) of 2 MPa. The brittle-ductile boundary is located at a depth of 20 km. The ductile lower crust is thick and has a Maxwell viscoelastic rheology phenomenologically described by a spring and a dashpot in series. Therefore, the modeled lower crust can accommodate time dependent creep strain. The shear relaxation time ( $\tau$ ) of the lower crust is assumed to be on the order of 10<sup>6</sup> years<sup>17</sup>. The crust is underlain by a viscous asthenosphere with viscosity corresponding to a relaxation time on the order of 10<sup>10</sup> years. The western and eastern ends of the model are assumed to be constrained. A summary of the parameters used in the numerical model is given in Table 1.

The model starts 20,000 years ago and assumes that there are no flexural stresses in the crust (the assumption is shown in Fig. 4a) and that the stress state is isotropic, i.e.  $S_{Hmin}$  are equal to  $S_v$ . While this assumption is overly simplified, it allows us to focus on the stress changes during deglaciation may have induced. To account for the effect of pore pressure we are using effective stresses ( $\sigma$ ).

$$\sigma = S - P_p$$

The pore pressure is assumed to be hydrostatic. Subsequently, the ice sheet starts to shrink as shown in Fig. 6b. The huge late Weichselian ice sheet that covered

North Sea some 20,000 years ago<sup>18</sup> shrank to a much smaller ice sheet within about 5,000 years<sup>19</sup>, 11,000 years ago the ice sheet retreated to the current coastal line<sup>20</sup> and 9,000 years ago it has melted away entirely.

The findings of the numerical model confirm the rough predictions of the analytical model in that the Tampen Spur is subjected to compressive flexural stresses, and closer to the coast flexural stresses are extensional (Fig. 7). The transition from compressive to extensional stresses is located just east of Visund. More specifically,  $S_{Hmax}/S_v$  is highest on the west side of the Tampen Spur approaching 1.5 at a depth of 500 m. In the Tampen Spur itself,  $S_{Hmax}/S_v$  is rapidly decreasing towards the west, but still higher than 1. Closer to the coast  $S_{Hmax}/S_v$  reaches values as small as 0.6. These variations decrease with depth and are almost negligible at a depth of 3,000 m.  $S_{Hmin}/S_v$  shows the same trend as  $S_{Hmax}/S_v$ , i.e. it's highest to the west of Snorre and drops significantly towards the coast. Therefore, the model predicts a reverse faulting stress state in the Tampen Spur with a tendency to strike-slip faulting in Visund, since  $S_{Hmin}$  drops below  $S_v$ . Closer to the coast both horizontal stresses are predicted to be smaller than  $S_v$ . Of course, if compressional stresses existed in the crust prior to deglaciation as generally observed in intraplate regions<sup>21,22</sup> the stress state would be even more compressive west of the Viking Graben, but less extensional east of it.

In Fig. 8a we show the change of stress with time as the ice sheet is melting. 15,000 years ago horizontal stresses are highly extensional in the area between the Viking Graben and the coast, which is the result of the rapid melting of the huge late Weichselian ice sheet<sup>18</sup> to a much smaller continental ice sheet<sup>19,20</sup>. The subsequent melting of the continental ice sheet diminishes the extensional stresses between the coast and the Viking Graben and causes compressive stresses in the Tampen Spur, which is characteristic for the present day stress field.

By looking at the relative magnitudes of  $S_{west-east}$  and  $S_{north-south}$  we can also make a rough prediction for the orientation of  $S_{Hmax}$  (Fig. 8b). If  $S_{west-east}$  is larger than  $S_{north-south}$ ,  $S_{Hmax}$  is striking parallel to the modeled cross section. On the other hand if  $S_{west-east}$  is smaller than  $S_{north-south}$ ,  $S_{Hmax}$  is perpendicular to the cross section. The model therefore predicts a change of the direction of  $S_{Hmax}$  from SEE-NWW striking on the western side of the Viking Graben, to NNE-SSW striking towards the coast. Preliminary results from the analysis of wellbore failure in block 35/9 show, that the  $S_{Hmax}$  orientation in fact is rotated relative to the orientation of  $S_{Hmax}$  in the Tampen Spur (pers. com. D. Wiprut 1998). However, the observed rotation is much smaller than predicted by the deglaciation model, which indicates that ridge push contributes to the local stress field. By adding a SEE-NWW striking compression ridge push is expected to diminish the rotation predicted by the deglaciation model.

### Discussion of results

The model shown in Figs. 6-8 is capable of explaining several features of the observed stresses in the northern North Sea. It predicts a compressive stress state in the Tampen Spur with

$S_{Hmin}$  close to or even higher than  $S_v$ . This is in good agreement with off test data that suggest  $S_3$  is very close to  $S_v$ . The modeled decrease of the horizontal stresses towards the coast can be seen in the leak-off data as well. The model predicts that the largest stress perturbations occur at shallow depth, but the leak-off data are perturbed to a depth of approximately 1,000 m.

It is hard to compare the modeled results with the available data, as there is almost no data available so far from observations of wellbore failure in the Tampen Spur which suggest a  $S_1/S_v$  of around 1.25 at a depth of 500 m. These are matched well by this model. The earth mechanics confirm the general trend from extensional to compressive stresses, i.e. reverse faulting in the Tampen Spur and extensional horizontal stresses closer to the coast, although the latter are generally poor. The model seems to underestimate the horizontal stresses in the proximity of the coast, as they are below  $S_v$ , but no normal faulting is observed. As mentioned earlier, modeled stresses are predicted to be low, because the model doesn't take into account ridge push.

The high pore pressures in the Tampen Spur and the elevated horizontal stresses in this area. Closer to the coast where the horizontal stresses are smaller, they are almost hydrostatic. This close relationship between horizontal stress and pore pressure suggests that part of the pore pressure in the Tampen Spur is caused by a poroelastic response to elevated horizontal stresses.

Obviously the model has several shortcomings. First, since we are only looking at stresses caused by ice rebound. Other stress sources such as ridge push and erosion are of great importance. We are also ignoring the cause erosion of the glaciated areas and sea level rise at the ice sheet rims<sup>23</sup>. Similarly to melting of ice sheets, the transition to a differential isostatic response and extensional flexural stresses as well. Furthermore, by using a two-dimensional model, we are ignoring the complex structure of the ice sheet. This might be important since 20,000 years ago the change in ice sheet extent was largest towards the northwest (Fig. 1). Also, since we start from an initially isotropic stress state, we are ignoring the field stresses caused by ridge push. Nevertheless, the model can explain high compressive stresses in the Tampen Spur and decreased horizontal stresses on the western side of the Viking Graben just by considering the melting of ice sheets. This indicates that deglaciation is an important stress source.

### Conclusions

1. The combination of available observations and the model shows that the present day stress field is reverse faulting in the Tampen Spur (i.e.,  $S_{Hmax} > S_v$ ) and less compressive on the east side of the Tampen Spur (i.e.,  $S_{Hmin} < S_v$ ).

2. The comparison of observed stresses and the model shows that deglaciation influences the stress field in the northern North Sea by increasing horizontal stresses on the west side of the Viking Graben, and decreasing horizontal stresses on the eastern side.

3. According to the numerical model, the regionally consistent NEE-SWW striking orientation of  $SH_{max}$  is expected to be rotated by 90 degrees in the proximity of the coast, e.g. block 35/9. However, the preliminary results of an analysis of wellbore failure show that the rotation is much smaller than predicted, thus indicating that ridge push contributes to the local stress field as well.

4. To a depth of 3,000 m the pore pressures are hydrostatic on the east side of the Viking Graben, but severely overpressured on the western side. The model suggests that this overpressure might be due to the poroelastic response to flexural stresses caused by deglaciation.

## Nomenclature

- $P_p$  = Pore pressure,  $m/Lt^2$ , MPa  
 $S_1$  = Maximum principal stress,  $m/Lt^2$ , MPa  
 $S_2$  = Intermediate principal stress,  $m/Lt^2$ , MPa  
 $S_3$  = Least principal stress,  $m/Lt^2$ , MPa  
 $S_v$  = Vertical stress,  $m/Lt^2$ , MPa  
 $SH_{max}$  = Maximum horizontal stress,  $m/Lt^2$ , MPa  
 $SH_{min}$  = Minimum horizontal stress,  $m/Lt^2$ , MPa  
 $\sigma$  = Effective stress,  $m/Lt^2$ , MPa  
 $\mu$  = Coefficient of friction  
 $C_0$  = Cohesion,  $m/Lt^2$ , MPa  
 $\rho$  = Density,  $m/L^3$ ,  $kg/m^3$   
 $E$  = Young's Modulus,  $m/Lt^2$ , GPa  
 $\nu$  = Poisson's ratio  
 $\tau$  = Maxwell relaxation time, t, years

## Acknowledgments

We would like to thank Norsk Hydro for generously providing the data and financial support for this study.

## References

- Wiprut, D.J., and Zoback, M.D.: "High Horizontal Stress in the Visund Field, Norwegian North Sea: Consequences for Borehole Stability and Sand Production," paper SPE 47244, this volume.
- Müller, B., Zoback, M.L., Fuchs, K., Mastin, L., Gregersen, S., Pavoni, N., Stephansson, O., Ljunggren, C.: "Regional Patterns of Tectonic Stress in Europe," *JGR* (1992) 97:B8, 11,783-11,803.
- Goelke, M., and Brudy, M.: "Orientation of Crustal Stresses in the North Sea and Barents Sea Inferred from Borehole Breakouts," *Tectonophysics* (Dec. 1996) Vol. 266, No. 1-4, 25-32.
- Zoback, M.D., Barton, C., Brudy, M., Chang, C., Moos, D., Peska, P., Vernik, L.: "Review of Some New Methods for Determining the In Situ Stress State from Observations of Borehole Failure with Applications to Borehole Stability and Enhanced Production in the North Sea," presented at the 1995 Workshop on Rock Stresses in the North Sea, Trondheim, Norway.
- Lindholm, C.D., Bungum, H., Villagram, M., and Hicks, E.: "Crustal Stress and Tectonics in Norwegian Regions Determined from Earthquake Focal Mechanisms," presented at the 1995 Workshop on Rock Stresses in the North Sea, Trondheim, Norway.
- Goelke, M.: "Patterns of Stress in Sedimentary Basins and the Dynamics of Pull-Apart Basin Formation," Thesis, Vrije Universiteit Amsterdam (1996).
- Forsyth, D., Uyeda, S.: "On the Relative Importance of Driving Forces of Plate Motion," *Geophysics* (1975) Vol. 43, 163-200.
- Bott, M.H.P., and Kusznir, N.J.: "The Origin of the Lithosphere," *Tectonophysics* (1984) Vol. 117, 1-14.
- Stein, S., Cloetingh, S., Sleep, N.H., Wortel, R.: "Earthquakes, Stresses and Rheology," *Earth and Planetary Science Letters* (1989), 231-259.
- Stephansson, O.: "Ridge Push and Glacial Rebound Generators in Fennoscandia," *Bull. Geol. Inst. Uppsala* (1988) N.S. Vol. 14, 39-48.
- Turcotte, D.L., and Schubert, G.: *Geodynamics*, Wiley-Interscience, New York City (1982).
- Carter, N.L., Tsenn, M.C.: "Flow Properties of the Lithosphere," *Tectonophysics* (1987) Vol. 136, 1-14.
- Kusznir, N.J., Bott, M.H.P.: "Stress Concentration in the Lithosphere Caused by Underlying Viscous Flow," *Tectonophysics* (1977) Vol. 43, 247-256.
- Zoback, M.D., Healy, J.H.: "Friction, Faulting and the Anisotropy of Crustal Stress," *Annals Geophysicae* (1984) Vol. 2, 689-698.
- Zoback, M.D., Healy, J.H.: "In Situ Stress Measurements at 10 km Depth in the Cajon Pass Scientific Reservoir," *Journal of Geophysical Research* (1990) Vol. 95, 5039-5057.
- Brudy, M., Zoback, M.D., Fuchs, K., Rasmussen, B., Baumgärtner, J.: "Estimation of the Complete Stress State at 10 km Depth in the KTB Scientific Drill Holes," *Journal of Geophysical Research* (1997) 102:B8, 18,453-18,463.
- Fjeldskaar, W.: "Flexural Rigidity of Fennoscandia and the Postglacial Uplift," *Tectonics* (1997) Vol. 16, 103-114.
- Andersen, B.G.: "Late Weichselian Ice Sheet Extent in Greenland," *The Last Great Ice Sheets* (1981), 103-114.
- Lundqvist, J.: "Late Weichselian Glaciation and Deglaciation in Scandinavia," *Quaternary Science Reviews* (1992) 11, 292.
- Mangerud, J., Larsen, E., Longva, O., and Thorsnes, E.: "Glacial History of Western Norway 15,000-10,000 Years Ago," *Boreas* (1979) Vol. 8 Nr. 2, 179-187.
- Zoback, M.D., Zoback, M.L.: "Tectonic Stress Fields in North America and Relative Plate Motions," *Neotectonics of North America*, Slemmons Engdahl Zoback and Blackwell (1991).
- Zoback, M.L.: "First- and Second-Order Patterns of Crustal Stress in the Lithosphere: The World Stress Map Project," *Journal of Geophysical Research* (1992) 97, 11,703-11,728.
- Riis, F., Fjeldskaar, W.: "On the Magnitude of and Quaternary Erosion and its Significance in Scandinavia and the Barents Sea," *Structural Geology and its Applications to Petroleum Geology*, Brekke Larsen Talleraas (eds.), NPF Special Publication 1992, Elsevier, Amsterdam (1992).

TABLE 1 - PARAMETERS USED FOR NUMERICAL MODEL

Depth unit	$\rho$ (kg/m <sup>3</sup> )	$E$ (GPa)	$\nu$	$t$ (years)	$\mu$	$C_0$ (MPa)
Upper crust (sediments)	2,350	35	0.25		0.6	2
Upper crust (basement)	2,700	56	0.25		0.6	2
Lower crust	2,900	71	0.25	100,000		
Mantle	3,300		0.25	10,000		

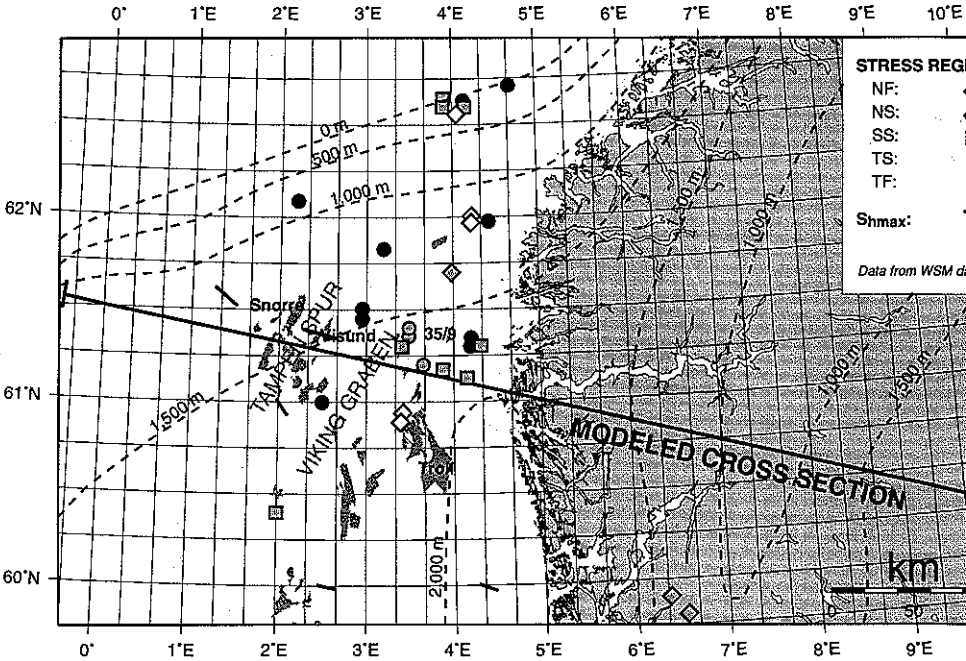


Fig. 1 Location map of the northern North Sea. Earthquake epicenter locations are plotted for different stress states.  $S_{Hmax}$  orientation of  $S_{Hmax}$ . The data is mostly from the World Stress Map database. The  $S_{Hmax}$  orientation in Visund is deduced from 'tensile fractures'. The dashed lines illustrate extent and thickness of the ice sheet 20,000 years ago<sup>18</sup>. The cross-section where the model is performed. The data in subsequent figures are also plotted along the same cross section.

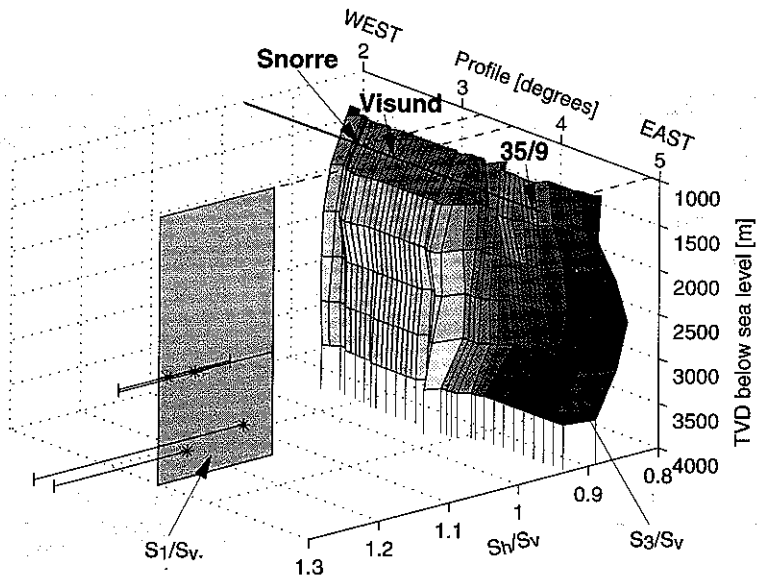


Fig. 2 Depth dependence of horizontal stresses, normalized by  $S_v$  along the cross section shown in Fig. 1. The plot shows the analysis of leak-off tests ( $S_3$ ), as well as the magnitudes of  $S_1$  from observations of wellbore failure in Visund'. Note  $S_3/S_v$  towards the coast.

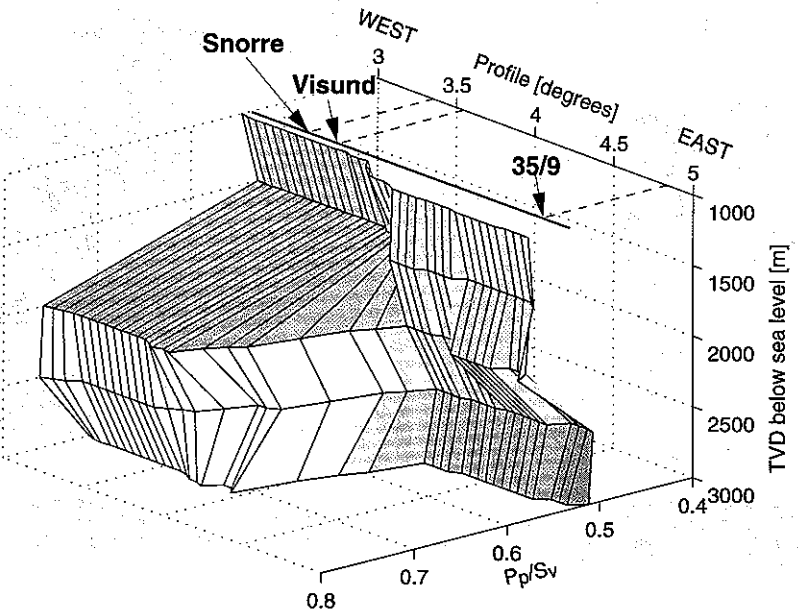
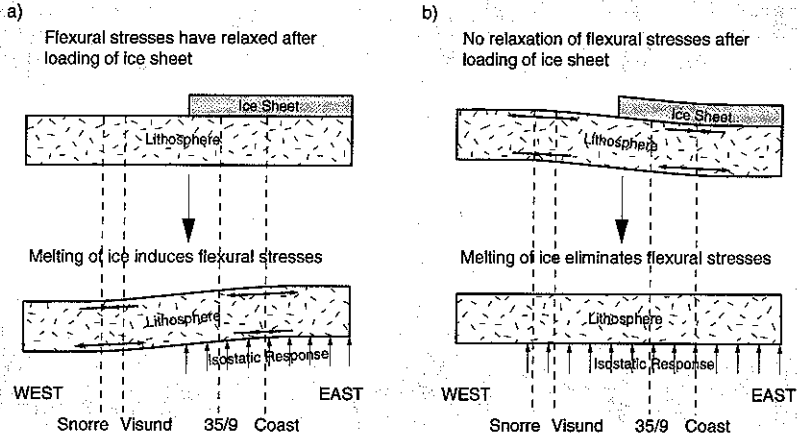
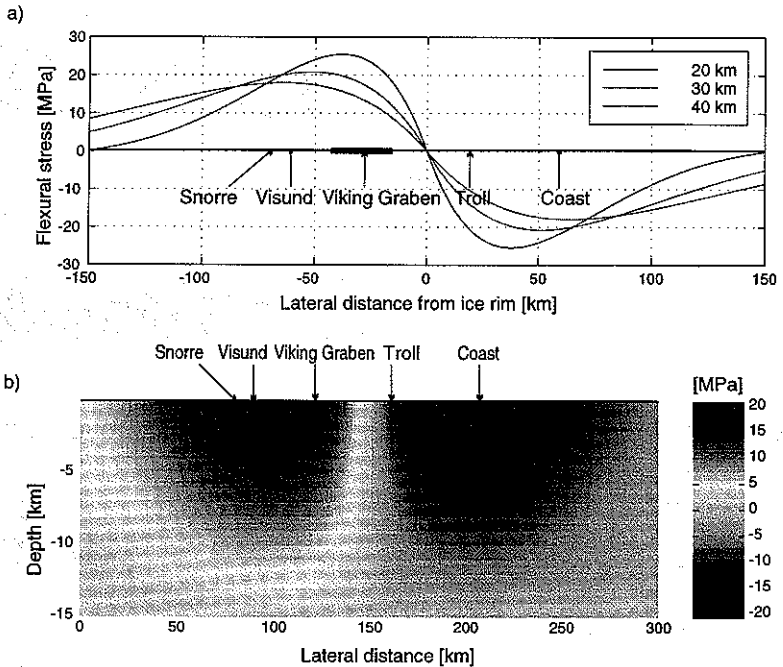


Fig. 3 Depth dependence of pore pressure, normalized by  $S_v$  along the cross section shown in Fig. 1. The majority of measurements are from RFT logs. The pore pressure is almost hydrostatic around block 35/9, but overpressured in the Tamp

**Flexurally Induced Stresses**



**Fig. 4** Illustration of flexural stresses caused by deglaciation. Fig. 4a shows expected flexural stresses for the assumption of Stephansson et al.<sup>9</sup>, that the lithosphere was in stress equilibrium before the ice sheet started to melt. Fig. 4b shows Stephansson's assumption that the lithosphere has not reached a stress equilibrium during the existence of the ice sheet.



**Fig. 5** Analytical model of stresses as a result of the flexure of an elastic plate<sup>11</sup>. Fig. 5a shows expected flexural stress as a function of the distance from the former ice sheet. The stresses are plotted for different elastic thicknesses of the lithosphere. Fig. 5b shows a plot of the change of flexural stresses with depth, for an assumed elastic thickness of 30 km.

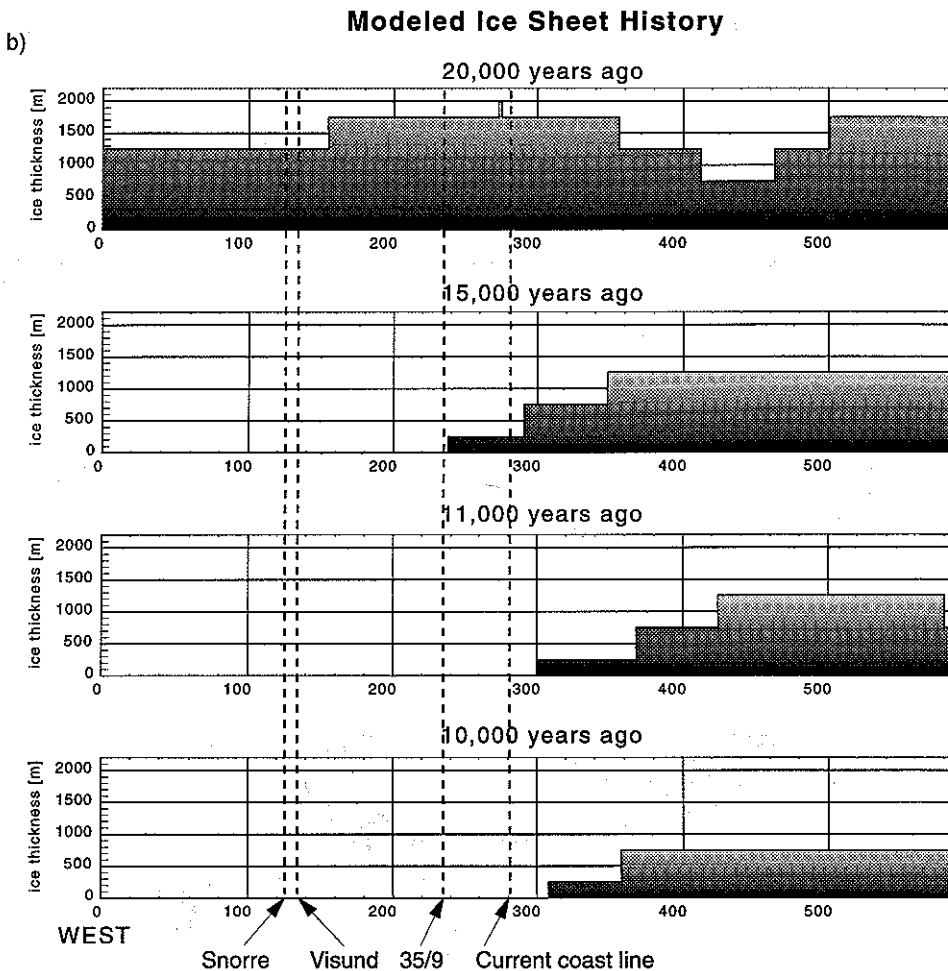
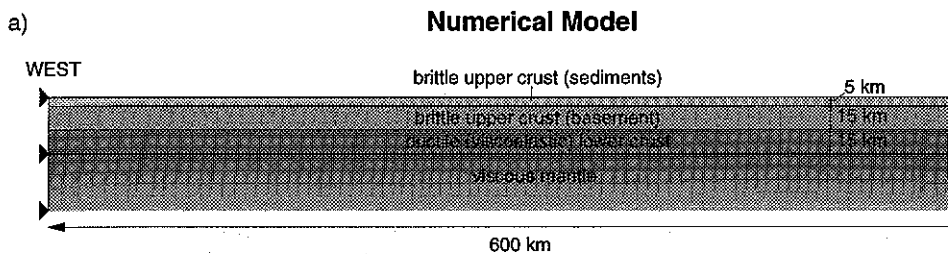


Fig. 6 Setup of the numerical model. Fig. 6a shows assumed rheologies and the geometry of the crust-mantle system used in the numerical model. Fig. 6b illustrates the change of the modeled ice sheet with time<sup>16,19,20</sup>. 9,000 years ago the ice sheet is melted.



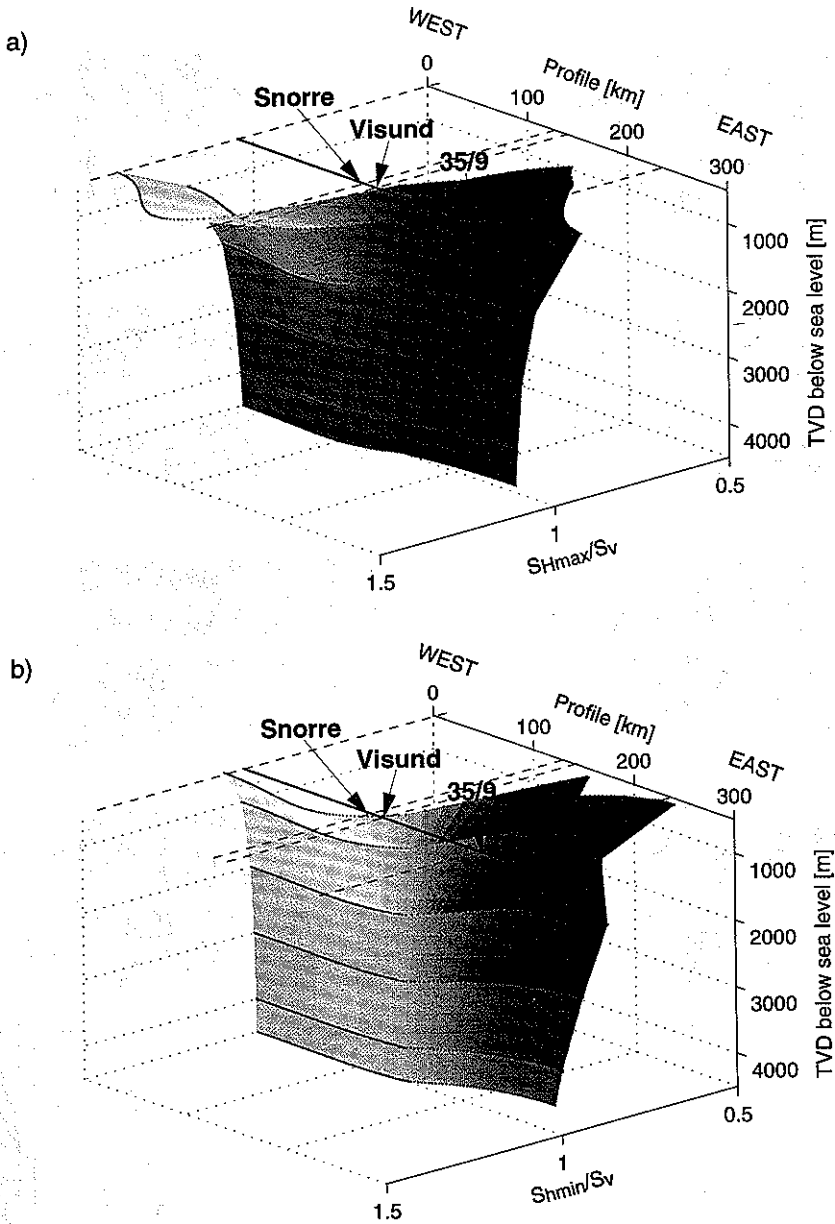


Fig. 7 Results for predicted present day magnitudes of  $S_{Hmax}$  and  $S_{Hmin}$  from the numerical model, plotted along the profile as Fig. 2 and Fig. 3 as a function of depth. Fig 7a shows that  $S_{Hmax}/S_v$  is high in the Tampen Spur and decreases towards the east of the Viking Graben.  $S_{Hmin}/S_v$  is plotted in Fig. 7b. Note the strong decrease of  $S_{Hmin}/S_v$  to the east of the Viking Graben.

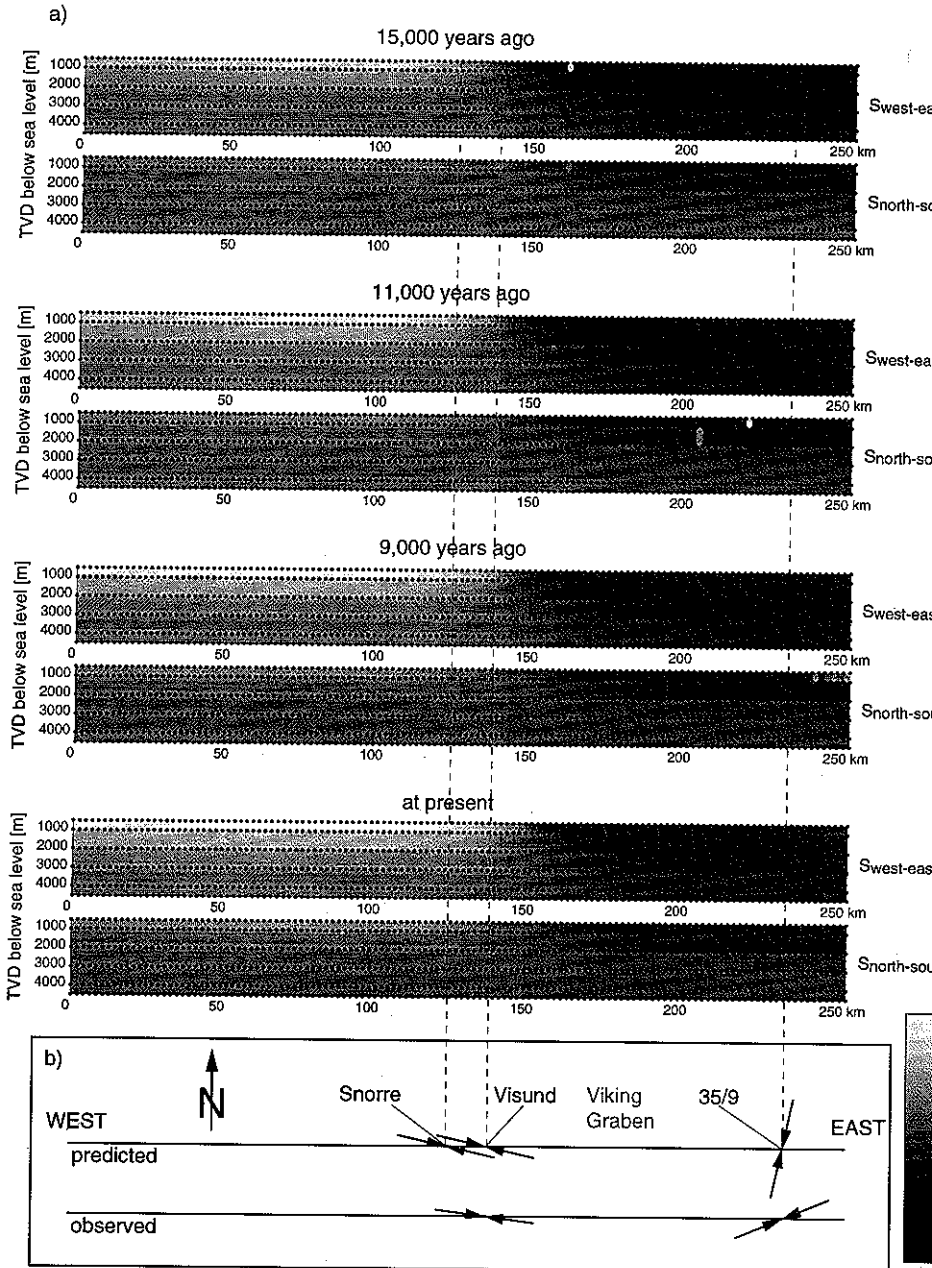


Fig. 8 Predicted change of horizontal stresses due to deglaciation (Fig. 8a) and implications for the orientation of  $S_{Hmax}$ . 15,000 years before present, horizontal stresses show a steady increase. At present horizontal stresses are higher than the the west side of the Viking Graben, but still lower on the east side. Since in block 35/9  $S_{west-east}$  is smaller than  $S_{north-south}$ , orientation of  $S_{Hmax}$  rotates by 90 degrees.